

High-Efficiency GaN Doherty Power Amplifier based on Inverse Class-F Operation

Anna Piacibello

*Department of Electronics and Telecommunications
Politecnico di Torino
Torino, Italy
anna.piacibello@polito.it*

Vittorio Camarchia

*Department of Electronics and Telecommunications
Politecnico di Torino
Torino, Italy
vittorio.camarchia@polito.it*

Abstract—This paper presents the design and characterization of a Doherty power amplifier based on high-efficiency continuous inverse class-F individual amplifiers. The prototype achieves a saturated output power in excess of 42.5 dBm, with efficiency higher than 70% and 50%, at saturation and 6 dB output back-off respectively, over the frequency band 1.45 GHz–1.75 GHz (18% fractional band). The good agreement between simulations and measurements and the comparison with the state of the art at similar frequencies demonstrate the potential of the application of harmonic tuning strategies to the Doherty architecture, despite the challenge of maintaining wideband operation.

Index Terms—Base station, Broadband, Doherty, Harmonic tuning, High efficiency, Power amplifier, 5G.

I. INTRODUCTION

The Doherty power amplifier (DPA) has gained widespread popularity as the preferred solution for radio frequency power amplifiers in communication bands below 6 GHz [1]. Its success can be attributed to the relatively simple design and the robustness it exhibits, especially over relatively narrow operating bandwidths.

Common design strategies for fully analog (single input) broadband DPA architectures include the utilization of class-AB stages [2] for the Main, along with class-C stages for the Auxiliary, low-order matching networks, and symmetrical configurations to ensure matching and phase alignment between the two branches across the desired operational bandwidth, as in [3], [4]. This, however, calls for a trade-off with the maximum achievable efficiency, which is typically lower for class-AB and class-C PAs compared to harmonically tuned PAs.

Moreover, if very wide bandwidths are required, it may be necessary to consider specific system-level solutions, such as adopting separate RF inputs for the Main and Auxiliary branches [5]–[7], to drive the two branches with stimuli having optimal phase and magnitude over frequency. However, these approaches can potentially diminish the benefits in terms of simplicity and robustness of the traditional DPA implementation.

Incorporating single-device harmonically-tuned PAs such as the class F/F⁻¹ [8]–[10] as building blocks in a DPA architecture [11]–[13], is very attractive due to their ability to achieve superior efficiency at saturation. However, this strategy faces certain limitations, primarily concerning the

need to maintain correct load modulation over the bandwidth, especially in single input DPAs. This often requires wideband parasitic compensation and a proper output combiner. To ensure matching and phase alignment between the branches across the working band, low-order matching networks are often adopted in DPAs. This approach contrasts with the high-order matching networks necessary at both the fundamental and harmonic frequencies, which are typical of harmonically-tuned stages [14]. As a result, incorporating harmonically-tuned PAs in a DPA topology can pose significant challenges.

In this paper, we exploit a continuous mode inverse class-F PA, originally designed for standalone operation, to operate in a DPA architecture. designed to cover FR1 5G frequency bands around 1.6 GHz. The prototype demonstrates good performance, achieving a saturated output power exceeding 42.5 dBm in the 1.45–1.9 GHz band. At saturation, the efficiency is higher than 70%, and at 6 dB output back-off (OBO), it is higher than 50% over the frequency band 1.45 GHz–1.75 GHz. The comparison between simulation and measurements validates the design approach, and the results are in line with the state of the art at similar frequencies.

II. DESIGN STRATEGY

To synthesize the Doherty architecture using a previously designed inverse class-F PA, which was matched to 50 Ω both at the input and output and intended for standalone operation in the 1.4–2 GHz range [15], some considerations are necessary. The output combiner can be designed on 50 Ω as shown in Fig. 1(a), which proves sufficient to cover the target band. Two branch amplifiers based on the original inverse class-F one will be used. The highly efficient operation enabled by the harmonic tuning will be mainly exploited in the Main branch.

For the correct Doherty operation to take place, however, it is necessary to verify whether the output matching network (OMN) of the individual PA is suitable to operate under load modulation or to modify it to make it so. In this case, the OMN did not originally introduce a phase rotation that is a multiple of 180°, and a delay line on $Z_{\text{out}} = 50 \Omega$ at the output is the simplest way to achieve this condition, although a relatively narrowband one. Its electrical length θ_{out} can be tuned to achieve the desired condition at a specific frequency in the operating band. The phase rotation of the OMN vs. frequency

is verified to be around 180° over its bandwidth (1.4–2 GHz), hence introducing a significant spreading which will likely hamper the correct Doherty operation over the whole band. In fact, after the insertion of an appropriate delay line, the OMN is verified to maintain the desired harmonic loading conditions regardless of the impedance modulation applied at its output, while properly modulating the fundamental load of the transistor only in a neighbourhood of the selected design frequency.

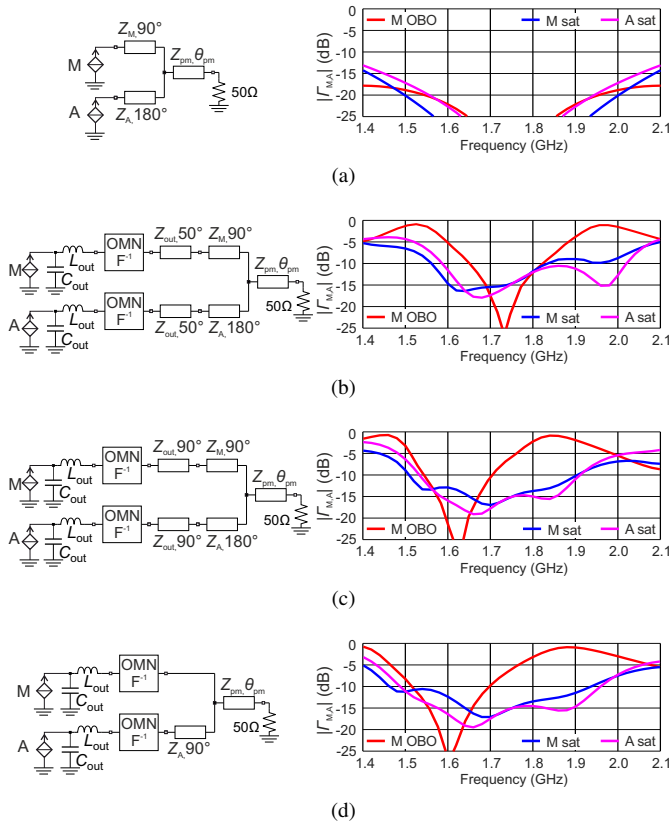


Fig. 1. Normalized load impedances synthesized at the current generator plane: (a) by the combiner only, (b) by the complete output section tuned at center frequency, (c) by the complete output section tuned at 1.6 GHz and (d) by the reduced output section tuned at 1.6 GHz. The values common to all cases are: $C_{out}=1.4$ pF, $L_{out}=1.2$ nH, $Z_M=Z_A=Z_{out}=50 \Omega$, $Z_{pm}=35 \Omega$, $\theta_{pm}=90^\circ$. All electrical lengths are referred to 1.75 GHz

The output section of the DPA is simulated assuming linear current stimuli with a 90° phase difference for the Main and Auxiliary branches, whose output parasitic effects are modelled by an equivalent $C_{out}-L_{out}$ model, as shown in Fig. 1. The loading condition at the current generators is estimated as $Z_{M,A} = V_{M,A}/I_{M,A}$ and represented as a reflection coefficient $\Gamma_{M,A}$ by normalizing the impedance to the ideal value at center frequency. The plots on the right correspond to $|\Gamma_{M,A}|$, at 6 dB OBO and at saturation. As anticipated, the combiner alone, when no output parasitic effect and no OMN is considered, is fully capable to cover the target band; the $|\Gamma_{M,A}|$ are all well below -10 dB.

To restore the appropriate phase delay at the original center frequency 1.75 GHz, the required delay line on $Z_{out} = 50 \Omega$

has an electrical length of $\theta_{out} = 50^\circ$ (Fig. 1(b)). The combiner response clearly shows that the load modulation can only be maintained on a narrower band (around 200 MHz), since the back-off loading condition of the Main deviates significantly from the desired one at the band edges.

If the delay line is tuned to center the DPA operation around 1.6 GHz (Fig. 1(c)), the required θ_{out} is 90° . The Main back-off loading condition shifts to lower frequencies, and the loading conditions of both branches at saturation also improve slightly. Besides, this configuration is advantageous since it allows simplifying the combiner, as shown in Fig. 1(d). In fact, since $Z_M=Z_A=Z_{out}=50 \Omega$, a 180° phase shift can be omitted in each branch. This reduces the size of the output combiner while allowing a slightly more wideband operation and ensuring very good loading conditions at saturation. Therefore, the latter configuration is selected for the integrated DPA implementation.

Another aspect to be considered when estimating the bandwidth of a DPA is related to the effect of the Auxiliary branch when it is off (below threshold). Theoretically, it should present an open circuit to the common node of the combiner, to avoid interfering with the Main operation in the low-power region. However, the high order of the OMN filter and the consequent large phase rotation over the band which was previously evidenced, also pose a limitation in this respect. Fig. 2 shows the normalized impedance presented by the Auxiliary at the common node in the selected configuration, i.e., with a 90° delay line. It is a good open circuit around 1.6 GHz, as expected, but it deviates rapidly away from it until it becomes close to a short circuit at 1.4 GHz and 1.9 GHz. Therefore, in terms of small-signal performance, the bandwidth of the DPA will be limited to such a range.

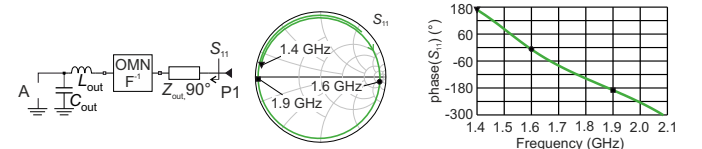


Fig. 2. Impedance presented at the common node of the DPA combiner by the Auxiliary when off.

The DPA architecture is then completed by including the input section, which is comprised of an even power splitter, two symmetric input matching networks (IMNs) and the appropriate phase alignment. The IMNs are analogous to the one of the single-stage inverse class-F PA apart from the layout. They ensure stability in and out of band, minimum reflections at the fundamental frequencies, and present a reactive impedance providing the optimum trade-off between efficiency and AM/AM at the second harmonic frequencies [16]. The even input splitter is designed on 50Ω adopting a single-section Wilkinson topology, and a 50Ω , 90° delay line is inserted on the Main branch.

III. FABRICATION AND CHARACTERIZATION RESULTS

The DPA is fabricated on a Rogers 4350B substrate with 3.66 relative dielectric constant, 0.762 mm thickness and 35 μm metal thickness. The layout is optimized for compactness, leading to an overall size of $140 \times 75 \text{ mm}^2$. The photograph of the realized prototype, mounted on an aluminum carrier for heat dissipation, is shown in Fig. 3.

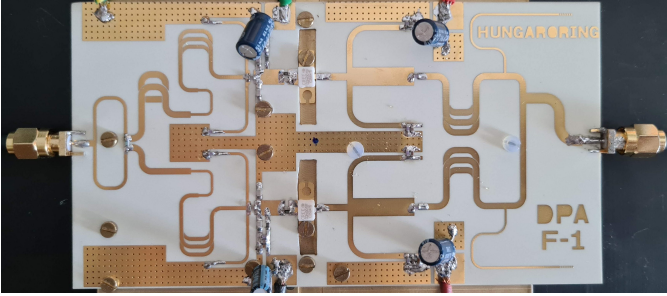


Fig. 3. Photograph of the inverse class-F DPA prototype.

The PA is characterized in small and large signal conditions at the nominal bias $V_{\text{DD}} = 28 \text{ V}$, $V_{\text{GM}} = -2.75 \text{ V}$, $V_{\text{GA}} = -6 \text{ V}$, corresponding to a quiescent drain current $I_{\text{D}} = 30 \text{ mA}$.

The small signal performance from 0.5 GHz to 3.5 GHz is reported in Fig. 4, where measured results (symbols) are compared to simulated ones (solid) showing good agreement, apart from a 50 MHz shift of the measurements toward low frequency. The measured input and output return loss result below 6 dB and 10 dB, respectively, and the associated gain is higher than 10 dB from 1.45 GHz to 1.9 GHz.

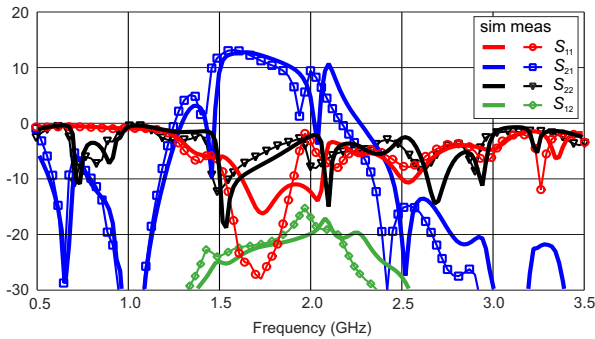


Fig. 4. Simulated (solid) and measured (symbols) scattering parameters.

The continuous wave (CW) large signal characterization is performed in the 1.45–1.9 GHz range using a real-time vector test bench, which is calibrated using a 2-port Short-Open-Load-Thru (SOLT) routine, along with an additional SOL calibration at an extended port connected to a power meter for absolute power calibration. Fig. 5 shows the comparison between the simulated power sweep at 1.65 GHz and the measured one at 1.6 GHz, according to the identified shift, likely due to tolerances and mechanical mounting of the active devices. The efficiency (η), power-added efficiency (PAE), and gain (G) versus output power all show an excellent agreement

between simulation and measurement. In the 6 dB OBO region, η and PAE are higher than 70% and 60%, respectively. This demonstrates the effectiveness of the proposed approach.

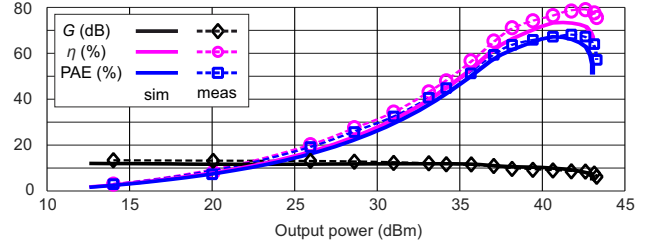


Fig. 5. CW performance vs. output power: simulated (solid) at 1.65 GHz and measured (symbols) at 1.6 GHz.

Fig. 6 summarizes the output power, gain and efficiency CW performance versus frequency. At saturation (5–6 dB gain compression), the output power is in excess of 42.5 dBm from 1.45 GHz to 1.9 GHz, with associated η higher than 70%. The bottleneck for bandwidth is the 6 dB OBO efficiency, as expected. It is higher than 50% in a 250 MHz range around the design frequency, in agreement with the prediction of the linear analysis of Fig. 1(d), and it is maintained above 30% over the full band from 1.45–1.9 GHz.

The adoption of a high-efficiency design strategy is evident at saturation, the benefits of the inverse class-F approach being slightly less pronounced at 6 dB OBO due to the non-optimal loading conditions imposed by the combiner. Nevertheless, the achieved performance is in line with the current state of the art, as indicated in Table I.

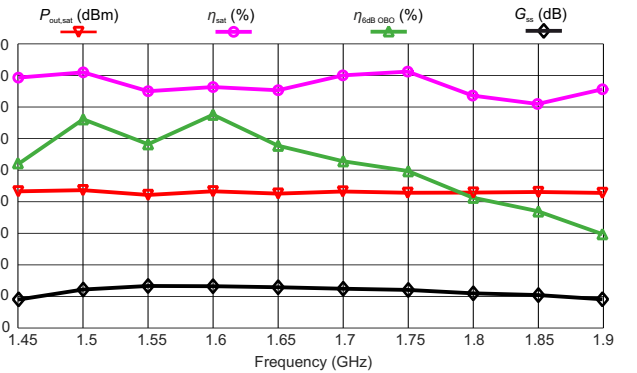


Fig. 6. Measured CW performance vs. frequency.

IV. CONCLUSION

A Doherty power amplifier based on a continuous inverse class-F PA has been designed for wideband operation, targeting the 5G FR1 bands around 1.6 GHz.

The design choices, including the combiner topology and phase alignment strategy, have been discussed, highlighting the key considerations for wideband operation. The fabricated demonstrator, achieves an output power higher than 42.5 dBm and corresponding efficiency exceeding 70%, over the frequency range of 1.45–1.75 GHz. At 6 dB back-off, the

TABLE I
COMPARISON WITH THE STATE OF THE ART.

Ref.	Technique	Freq. (GHz)	P_{sat} (dBm)	η_{sat} (%)	η_{OBO} (%)
[11]	DPA	2.14	35	55	50
[12]	DPA	2–2.6	41.7–43.8	61–75	45–64
[17]	LMBA	1.8–3.8	44	46–70	33–49
[18]	PD-LMBA	1.5–2.7	42.5	58–72	47–61
[19]	CM-LMBA	1.45–2.45	45.6–46.7	67–78	51–64
[20]	LMBA	2.4	43	54	49
T. W.	DPA	1.45–1.75	42.5	75–80	50–68

efficiency and gain remain above 50% and 10 dB, respectively. The performance of the prototype aligns well with state-of-the-art PAs at similar frequencies and is accurately predicted by simulations, despite the achievable bandwidth is narrower than that of the original inverse class-F PA. Further work should address the design of wideband harmonically-tuned PAs for operation under load modulation.

ACKNOWLEDGEMENT

This research was supported by the Project Programma Operativo Nazionale (PON) Ricerca e Innovazione “Tecnologie abilitanti e architetture innovative per future generazioni (6G) di trasmettitori intelligenti green” (DM 1062/21, CUP E15F21003760001) funded by the Italian Ministry of University and Research (MUR).

REFERENCES

[1] V. Camarchia, M. Pirola, R. Quaglia, S. Jee, Y. Cho, and B. Kim, “The Doherty power amplifier: Review of recent solutions and trends,” *IEEE Trans. Microw. Theory Techn.*, vol. 63, no. 2, pp. 559–571, Feb. 2015.

[2] M. Iqbal and A. Piacibello, “A 5 W class-AB power amplifier based on a GaN HEMT for LTE communication band,” in *2016 16th Mediterranean Microwave Symposium (MMS)*, 2016, pp. 1–4.

[3] M. Yang, J. Xia, and A. Zhu, “A 1.8–2.3 GHz broadband Doherty power amplifier with a minimized impedance transformation ratio,” in *2015 Asia-Pacific Microwave Conference (APMC)*, vol. 1, 2015, pp. 1–3.

[4] A. Nasri, M. Estebarsari, S. Toofan, A. Piacibello, M. Pirola, V. Camarchia, and C. Ramella, “Design of a Wideband Doherty Power Amplifier with High Efficiency for 5G Application,” *Electronics*, vol. 10, no. 8, 2021.

[5] C. M. Andersson, D. Gustafsson, J. Chani Cahuana, R. Hellberg, and C. Fager, “A 1–3-GHz Digitally Controlled Dual-RF Input Power-Amplifier Design Based on a Doherty-Outphasing Continuum Analysis,” *IEEE Trans. Microw. Theory Techn.*, vol. 61, no. 10, pp. 3743–3752, 2013.

[6] A. Piacibello, R. Quaglia, V. Camarchia, C. Ramella, and M. Pirola, “Dual-input driving strategies for performance enhancement of a Doherty power amplifier,” in *2018 IEEE MTT-S International Wireless Symposium (IWS)*, 2018, pp. 1–4.

[7] A. Piacibello, M. Pirola, V. Camarchia, C. Ramella, R. Quaglia, X. Zhou, and W.-S. Chan, “Comparison of S-band Analog and Dual-Input Digital Doherty Power Amplifiers,” in *2018 13th European Microwave Integrated Circuits Conference (EuMIC)*, 2018, pp. 269–272.

[8] F. Raab, “Maximum efficiency and output of class-F power amplifiers,” *IEEE Trans. Microw. Theory Techn.*, vol. 49, no. 6, pp. 1162–1166, 2001.

[9] A. Grebennikov, “Load network design technique for class F and inverse class F PAs,” *High Frequency Electronics*, vol. 10, no. 5, pp. 58–72, 2011.

[10] P. Colantonio, F. Giannini, G. Leuzzi, and E. Limiti, “On the class-F power amplifier design,” *International Journal of RF and Microwave Computer-Aided Engineering*, vol. 9, no. 2, pp. 129–149, 1999.

[11] P. Colantonio, F. Giannini, R. Giofre, and L. Piazzon, “Efficiency improvement in Doherty power amplifier by using Class F approach,” in *2009 European Microwave Integrated Circuits Conference (EuMIC)*, 2009, pp. 17–20.

[12] F. Meng, Y. Sun, L. Tian, and X.-W. Zhu, “A broadband high-efficiency Doherty power amplifier with continuous inverse class-F design,” in *2017 XXXIInd General Assembly and Scientific Symposium of the International Union of Radio Science (URSI GASS)*, 2017, pp. 1–3.

[13] C. Wang, G. Deng, and Z. Cao, “A High-Efficiency Doherty Power Amplifier Design with Continuous Inverse Class-F,” in *2022 IEEE 10th Asia-Pacific Conference on Antennas and Propagation (APCAP)*, 2022, pp. 1–2.

[14] V. Carrubba, A. L. Clarke, M. Akmal, Z. Yusoff, J. Lees, J. Benedikt, S. C. Cripps, and P. J. Tasker, “Exploring the design space for broadband pas using the novel “continuous inverse class-F mod”,” in *2011 41st European Microwave Conference*, 2011, pp. 333–336.

[15] A. Piacibello, Z. Zhang, and V. Camarchia, “Continuous Inverse Class-F GaN Power Amplifier with 70% Efficiency over 1.4-2 GHz Bandwidth,” in *2023 IEEE Topical Conference on RF/Microwave Power Amplifiers for Radio and Wireless Applications*, 2023, pp. 10–12.

[16] T. Sharma, J. S. Roberts, S. K. Dhar, S. Shukla, R. Darraji, D. G. Holmes, and F. M. Ghannouchi, “On the Efficiency and AM/AM Flatness of Inverse Class-F Power Amplifiers,” in *2019 IEEE MTT-S International Microwave Symposium (IMS)*, 2019, pp. 460–463.

[17] P. H. Pednekar, E. Berry, and T. W. Barton, “RF-Input Load Modulated Balanced Amplifier With Octave Bandwidth,” *IEEE Trans. Microw. Theory Techn.*, vol. 65, no. 12, pp. 5181–5191, 2017.

[18] Y. Cao and K. Chen, “Pseudo-Doherty Load-Modulated Balanced Amplifier With Wide Bandwidth and Extended Power Back-Off Range,” *IEEE Trans. Microw. Theory Techn.*, vol. 68, no. 7, pp. 3172–3183, 2020.

[19] J. Pang, C. Chu, Y. Li, and A. Zhu, “Broadband RF-Input Continuous-Mode Load-Modulated Balanced Power Amplifier With Input Phase Adjustment,” *IEEE Trans. Microw. Theory Techn.*, vol. 68, no. 10, pp. 4466–4478, 2020.

[20] K. Vivien, P. E. de Falco, G. Baudoin, O. Venard, P. P. C. Felix, and T. Barton, “Load Modulated Balanced Amplifier Designed for AM-PM Linearity,” in *2020 50th European Microwave Conference (EuMC)*, 2021, pp. 304–307.